Grid Synchronization of WEC-PV-BES Based Distributed Generation System using Robust Control Strategy

Seema, *IEEE Member* and Bhim Singh, *IEEE Fellow*

Abstract- In this paper, a renewable (Solar and Wind) energy sources based distributed generation system (DGS) is controlled to operate in the grid connected mode and an islanded mode using the robust and fast IAPV (Improved Affine Projection Versoria) and proportional resonant (PR) based control strategy. Due to the use of IAPV based control in the grid connected mode, the grid current becomes immune to the DC offset and the other non-fundamental harmonics during an unbalanced load, which significantly improves the grid current quality. It also presents the flexible operation of DGS in the grid connected mode using the variable and constant power injection into the grid, which ensures the grid stability during large and fast wind and solar power variations. Moreover, a MSOS-FLL (Modified Second Order Sequence Frequency Locked Loop) is used to improve the synchronization and seamless mode switching (islanded to grid connected and vice versa) performance by quickly and accurately estimating the phase angle and frequency at distorted and unbalanced grid voltages. Simulation and test results validate the microgrid operation and robustness of the microgrid control.

Keywords: Distributed Generation System, Synchronization, Load converter, Machine Converter and Power Quality.

I. INTRODUCTION

Today, renewable energy sources (RESs) based distributed generation systems (DGSs) are gaining attention due to the availability of RESs in abundance [1]-[2]. The growth of RES based DGS, is motivated by environmental concerns due to setback of fossil fuel power plants. However, the RES based DGS poses some challenges such as voltage and frequency fluctuations in an islanded mode due to the intermittent nature of RES such as solar and wind [3]. Therefore, the storage battery is introduced in the RES based DGS in the islanded mode of operation. Alsaidan et. al. [4] and Datta et. al. [5] have reported the importance of a storage battery in an islanded DGS. Hence the RES based DGSs are capable to feed the local loads with high quality power. Regardless of all promising features, the DGS is still not a matured technology. Various control and operational issues are extensively investigated such as the grid synchronization control, in grid-connected mode, the stability and reliability, power management and voltage control in an islanded mode [6]-[10]. In the reported literature [11]-[14], various grid synchronization techniques are discussed in order to improve the control performance and to inject the high quality power in the grid. In the grid synchronization unit, the accurate phase angle detection technique plays a vital role in multifunctional DGS. In last few decades, various phase angle detection techniques are reported such as SRF-PLL (Synchronous Reference Frame- Phase Locked Loop), ANF (Adaptive Notch Filter) [13] and CDSC-PLL (Cascaded Delayed Signal Cancelation) [14]. Although, these reported techniques present phase angle detection approach when input voltages are distorted and unbalanced. However, this technique does not consider the mode of switching from an islanded mode to the grid-connected mode under nonlinear loading. Therefore, in presented DGS, the MSOS–FLL (Modified Second Order Sequence Frequency Locked Loop) is used to estimate the phase angle of the grid voltage and an individual synchronization technique is used to quick mode of switching from an islanded mode to the grid connected mode and vice versa. This phase angle estimator works well during frequency variation, which is advantageous in this MSOS-FLL. Along with synchronization technique, here a new grid-connected control is also presented to improve the performance of DGS in the grid-connected mode of operation under dynamic conditions.

Generally, an indirect current control is used to generate the switching pulses for the grid connected VSC (Voltage Source Converter) [15]. Substantial literature [16]-[21] have reported the indirect control. In an indirect current control, the reference grid currents are estimated by using the fundamental load current and other feedforward term in the solar grid connected system. Vishal et. al. [17] have discussed the filter, which is used to estimate the load current fundamental for the reference grid current estimation. However, the reported control techniques have some advantages over others control techniques. Such as SRF (Synchronous Reference Frame) [17] based control technique is robust and fast at normal condition, however, under DC-offset condition and unbalanced load currents, the performance of SRF control is affected. Moreover, similarly, PLL, EPLL [18], SOGI [19], advanced SOGI-PLL [20], and SOGI-FLL [21] based control techniques have some advantages and disadvantages. Therefore, in this paper, an IAPV (Improved Affine Projection Versoria) based adaptive VSC control algorithm with the improved feed-forward term is used in the grid-connected mode [22]-[23]. The IAPV has various advantages over the existing control techniques.

Along with fast, adaptive and robust filter for the grid connected mode, here an improved feed-forward term is also included to improve the dynamic response of the system. In grid-connected mode, the prime objective of IAPV control algorithm is to estimate the balanced and sinusoidal reference grid currents regardless of the operating conditions of the grid voltages. Moreover, here in the islanded mode of operation, the VSC (LC-Load Converter) control switches into the voltage control mode and it is based on PR (Proportional resonant) controller rather than the PI (Proportional Integral) control. Because the response and tracking capability of PI control, are not fast enough for AC quantities. Hence, this paper deals with multifunctional and multi-objective DGS. To show the main contribution of the

This article has been accepted for publication in a future issue of this journal, but has not been fully edited. Content may change prior to final publication. Citation information: DOI 10.1109/TIA.2020.3021060, IEEE Transactions on Industry Applications

TABLE I MICROGRID OPERATING MODES

References	Grid Connected Mode				Islanded Mode	Seamless mode switching
	Grid current quality improvement with DC-offset in load current	Grid current quality improvement during unbalanced load	Grid current quality improvement during abnormal grid voltage	Constant and variable power mode	Improved voltage quality during unbalanced load	Fast and seamless grid connection (within 2 cycle)
[24]	No	No	No	No	yes	No
[25]-[26]	No	Yes	No	Only variable power	No	No
[27]	No	No	No	No	Yes	No
[28]	No	Yes	No	Only variable power	No	No
[29]-[31]	No	Yes	No	Only variable power	No	No
[32]	No	Yes	No	Not mentioned	Yes	Mode Switching occur but no discussion regarding fast grid connection
[33]	No	No	No	No grid connected	Yes	No
[34]	No	Yes	No	Only variable power	No	No
[35]-[36]	No	Yes	No	Grid connected only	Yes	Yes
[37]	No	Yes	No	Only variable power	Yes	Manual Mode switching
[38]-[39]	No	Yes	No	Only variable power	No	No
[40]	No	Yes	No	Only variable power	Yes	Mode of Switching occur but no discussion regarding fast grid connection
[41]-[42]	No	Yes	No	Only variable power	No	No
[43]-[44]	No	No	No	No	Yes	No
Presented manuscript	Yes	Yes	Yes	Constant and variable power mode	Yes	Yes

paper, an exhaustive literature survey [24]-[44] has been presented in Table I. The main contributions of this work, are as follows.

- This distributed generation system (DGS) is operated in an islanded mode and the grid-connected mode based on grid availability and the fault in the grid.
- For the synchronization unit, the MSOS-FLL based phase angle estimator is used to improve the grid synchronization process and immune the synchronization process from the voltage distortion and frequency variation.
- In grid-connected mode, the improved affine projection versoria control algorithm is used to inject the solar and wind-generated active powers into the grid with an improved power quality. Moreover, the grid currents quality is protected against the DC-offset and load current harmonics.
- The solar power feed-forward term in the grid-connected mode is used to improve the dynamic response of DGS under fast and sudden variation in the solar irradiance.
- In grid fault condition, the DGS automatically switches to an islanded mode without any transient. Here, in an islanded mode of operation of DGS, the PR controller is used to achieve the balanced and sinusoidal CCP (Common Coupling Point) voltages. Therefore, the power quality of CCP voltages always remains well within the IEEE-1547 standard.

II. DGS CONFIGURATION

Fig.1 depicts a DGS (Distributed Generation System) configuration, which consists of a solar PV (Photovoltaic) array, a wind turbine driven SCIG (Squirrel Cage Induction Generator) with the energy storage battery. Here, the grid is connected at CCP (Common Coupling Point) of DGS through the solid state switches (Solid State Switches) as shown in Fig. 1. The boost converter is used to connect the solar PV array at DC-link of the LC (Load Converter) and delivers the solar generated active power to the DC-link. The wind turbine SCIG is controlled through MC (Machine Converter). Two R-C filters are used to reduce switching noise from the CCP voltages as shown in Fig.1.

III. CONTROL STRATEGY

The mode of DGS is switched using the converter control strategy. Here two converters are used one for the generator control and another is for load/grid power control. The load side converter (LC) controls voltage and frequency of islanded microgrid, the grid connection/disconnection control and grid power quality in the grid connected mode. The machine converter extracts the peak power from the wind generator and takes care the generator currents quality. Here, this DGS is operating in the grid-connected (GC) mode and an islanded mode (IM), in order to provide the uninterrupted power to the local loads. A robust control strategy is presented in this work, to operate DGS in IM and GC modes without any transient.

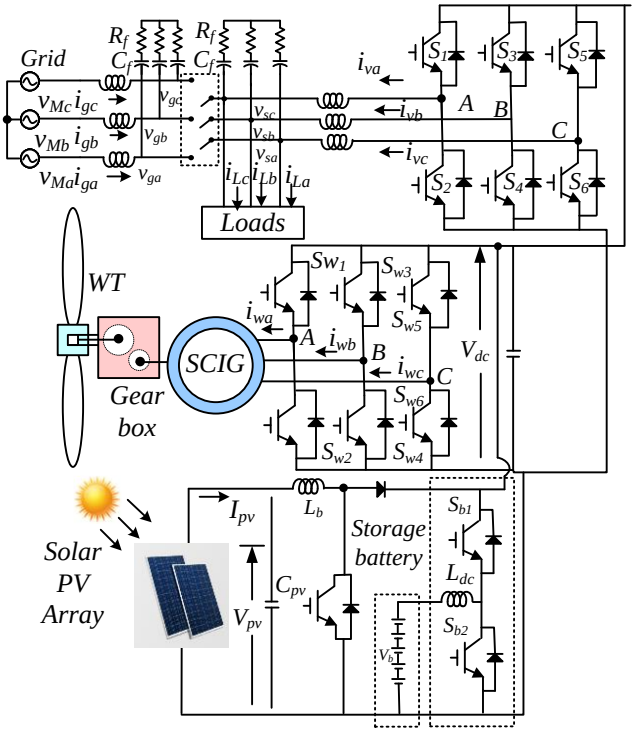

Fig. 1 Distributed generation system configuration

The presented control strategy is categorized into three parts (1) grid-connected mode as shown in Fig. 2, (2) an islanded mode and (3) the synchronization control. Here, in this DGS, a storage battery is used for active power balancing, which is connected at DC-link by using the bi-directional DC-DC converter (BDC) and the role of BDC in DGS is to control the DC-link voltage as

This article has been accepted for publication in a future issue of this journal, but has not been fully edited. Content may change prior to final publication. Citation information: DOI 10.1109/TIA.2020.3021060, IEEE Transactions on Industry Applications

shown in Fig. 3 and safe battery current even from second harmonic. The control algorithm of the DGS is described in the following subsections.

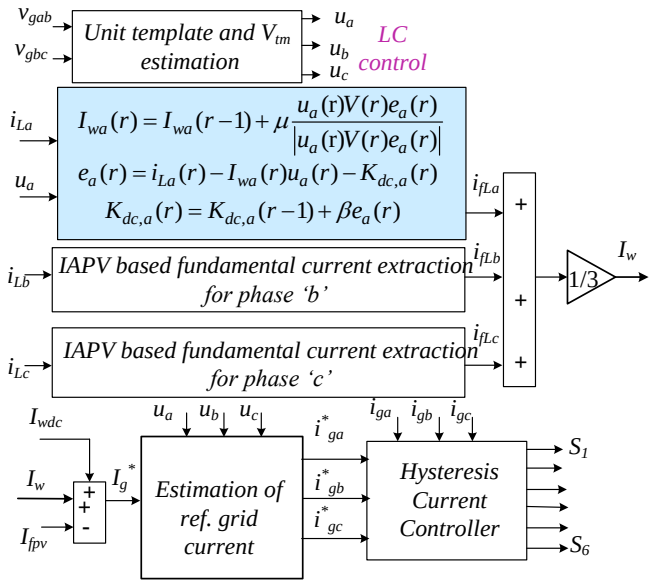

(a)

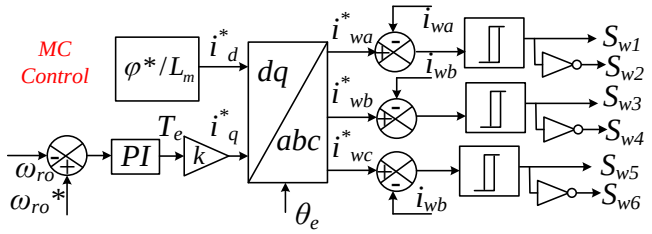

(b)

Fig.2 Grid connected control (a) for LC and (b) for MC

A. Grid-Connected Mode of DGS

In grid-connected mode, the switching pattern of LC is generated through an indirect current control. The indirect current control of LC, is based on IAPV (Improved Affine Projection Versoria) algorithm as shown in Fig.2(a). Here, the IAPV filter is used to estimate the reference grid currents to improve the grid currents quality at highly nonlinear load.

The load current fundamental component is estimated through IAPV algorithm. The IAPV control algorithm requires the in-phase component for computing the load current fundamental component, which is shown in Fig. 2(a).

The estimation of in-phase unit templates, is as follows,

$$u_a=\frac{v_{ga}^+}{V_t},u_b=\frac{v_{gb}^+}{V_t},u_c=\frac{v_{gc}^+}{V_t} \tag{1}$$

Where, v_{ga}, v_{gb} and v_{gc} are grid phase voltages. The grid phase voltages are computed through the following expression,

$$v_{ga}^+=\frac{1}{3}\left(2v_{gab}^++v_{gbc}^+\right),\quad v_{gb}^+=\frac{1}{3}\left(-v_{gab}^++v_{gbc}^+\right),\quad v_{gc}^+=\frac{1}{3}\left(-v_{gab}^+-2v_{gbc}^+\right) \tag{2}$$

Where, v_{gab}^+, v_{gbc}^+ are the positive sequence line voltages and these positive sequence voltages are estimated using the MSOS (Modified Second Order Sequence)-FLL as shown in Figs. 3-4 and following governing equations.

$$v_{gab}^+=\frac{1}{3}\left[\frac{1}{2}\left(v_{gbc}-v_{gca}\right)+v_{gab}\right]-\left[\frac{1}{2\sqrt{3}}\left(v_{gbc}+v_{gca}\right)\right] \tag{3}$$

$$v_{gca}^+=\left[\frac{1}{2\sqrt{3}}\left(v_{gab}-v_{gbc}\right)\right]-\frac{1}{3}\left[\frac{1}{2}\left(v_{gab}+v_{gbc}\right)+v_{gca}\right] \tag{4}$$

$$v_{gbc}^+=\left(-v_{gab}^+-v_{gca}^+\right) \tag{5}$$

Where, v_{gab}^+, v_{gbc}^+ and v_{gca}^+ are the positive sequence voltages. The fundamental active current component is estimated as [45],

$$I_{pa}(r)=I_{pa}(r-1)+\mu\frac{u_a(r)V(r)e_a(r)}{|u_a(r)V(r)e_a(r)|} \tag{6}$$

$$\text{Where } e_a(r)=i_{La}(r)-I_{pa}(r)u_a(r)-K_{dc,a}(r) \tag{7}$$

and μ is equal to .0025.

$$\text{And } K_{dc,a}(r)=K_{dc,a}(r-1)+\beta e_a(r) \tag{8}$$

Where, $K_{dc,a}$ is an adaptive variable to reject the DC-offset component.

Similarly, the active weight components of load currents for phase 'b' and 'c' are estimated as,

$$I_{pb}(r)=I_{pb}(r-1)+\mu\frac{u_b(r)V(r)e_b(r)}{|u_b(r)V(r)e_b(r)|} \tag{9}$$

$$e_b(r)=i_{Lb}(r)-I_{pb}(r)u_b(r)-K_{dc,b}(r) \tag{10}$$

$$I_{pc}(r)=I_{pc}(r-1)+\mu\frac{u_c(r)V(r)e_c(r)}{|u_c(r)V(r)e_c(r)|} \tag{11}$$

$$e_c(r)=i_{Lc}(r)-I_{pc}(r)u_c(r)-K_{dc,c}(r) \tag{12}$$

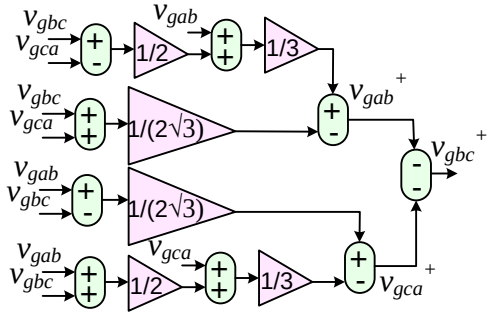

Fig. 3 Positive sequence estimator

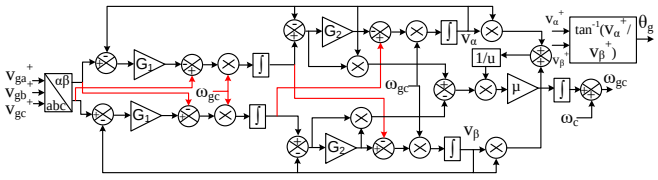

Fig. 4 MSOS-FLL block diagram

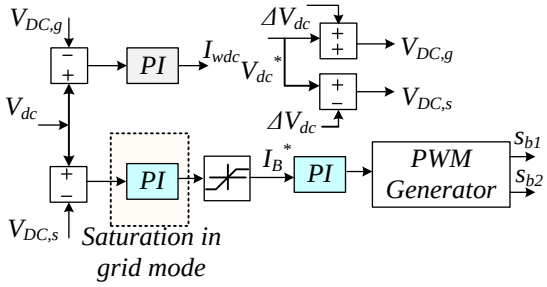

(a)

This article has been accepted for publication in a future issue of this journal, but has not been fully edited. Content may change prior to final publication. Citation information: DOI 10.1109/TIA.2020.3021060, IEEE Transactions on Industry Applications

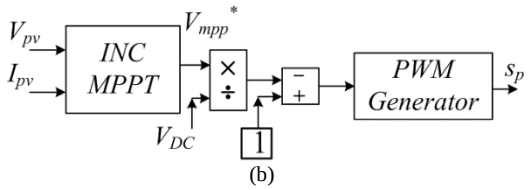

Fig. 5 BDC and solar PV array peak power control

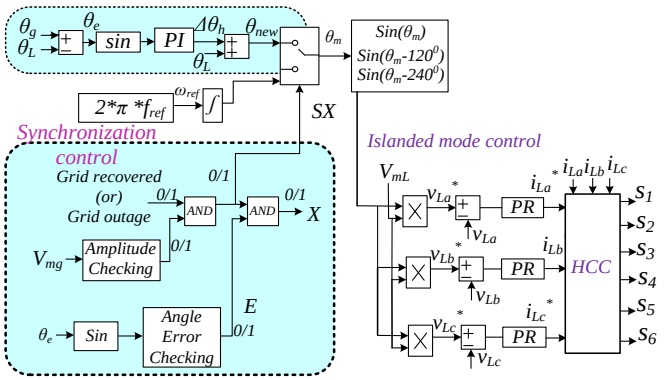

Fig. 6 Islanded mode of LC control

The average fundamental load current is estimated as,

$$I_p = \frac{I_{pa} + I_{pb} + I_{pc}}{3} \tag{13}$$

The reference grid current weight is computed as,

$$I_g^* = I_p + I_{dc} - I_{fpv} - I_{fwi} \tag{14}$$

Where, I_{dc} is a weight component for DC-link voltage control.

The common DC-link voltage is controlled through a PI controller, which is formalized in discrete time as,

$$I_{dc}(\mathrm{r}) = I_{dc}(\mathrm{r}-1) + k_p\{(V_e(\mathrm{r}) - V_e(\mathrm{r}-1)\} + k_i\{\mathrm{V}_e(\mathrm{r})\} \tag{15}$$

Where, V_e is error of reference DC-link voltage (V_{dc}^*) and the sensed DC-link voltage (V_{dc}).

I_{fpv} and I_{fw} are the PV power and wind power feed-forward terms, respectively. The PV feed-forward term is estimated as,

$$I_{fpv} = k\left(\frac{2P_{pv}}{3V_t}\right) \text{and } I_{fwi} = \left(\frac{2P_{wind}}{3V_t}\right) \tag{16}$$

Therefore, the response of the system is improved under dynamic condition.

The reference sinusoidal grid currents are estimated as follows,

$$i_{ga}^* = u_a \times I_g^*, i_{gb}^* = u_b \times I_g^*, i_{gc}^* = u_c \times I_g^* \tag{17}$$

The hysteresis current controller is used to generate the switching pulses of LC. The error of the hysteresis band is computed through reference and sensed grid currents. Fig. 2 (b) shows the MC control for extracting the wind peak power with improved power quality of SCIG. The MC control is based on an indirect vector control as shown in Fig. 2 (b).

Moreover, Fig. 5 shows the DC-link voltage regulation technique with solar peak power extraction control algorithm. The DC-link voltage regulation is achieved through the BDC (Bidirectional DC-DC Converter) in an islanded mode. However, in the grid connected mode, an outer PI (Proportional Integrator) is saturated and BDC switching pulses are achieved through the constant current mode and DC-link voltage regulation is achieved through the load converter.

In the grid connected mode, the outer PI controller is saturated and the battery reference current is equal to the lower saturation limit. The battery current PI controller is expressed as,

$$D(r) = D(r-1) + k_{pib}\left\{I_{be}(r) - I_{be}(r-1)\right\} + k_{ppb} I_{be}\ (\mathrm{r}) \tag{18}$$

Where, I_{be} is error between the reference and sensed battery currents. These k_{pib} and k_{ppb} are the gains of the PI controller.

B. Islanded Mode of DGS

In the islanded mode, the LC is used to generate the CCP voltages using the PR (Proportional Resonant) controller as shown in Fig. 6. The reference CCP voltage is given through the DSP (Digital Signal Processor) and reference voltage {V_{ref} = 230*√2/(√3)V} and frequency (f_{ref} = 50Hz). In an islanded mode, VSC control algorithm consists of three PR (Proportional Resonant) controllers. The outputs of PR controllers are expressed as [46],

$$i_{vsca}(\mathrm{r}) = n_o v_{ea}(\mathrm{r}) + n_1 v_{ea}(\mathrm{r}-1) + n_2 v_{ea}(\mathrm{r}-2) - d_1 i_{vsca}(\mathrm{r}-1) - d_2 i_{vsca}(\mathrm{r}-2) \tag{19}$$

$$i_{vscb}(k) = n_o v_{eb}(\mathrm{r}) + n_1 v_{eb}(\mathrm{r}-1) + n_2 v_{eb}(\mathrm{r}-2) - d_1 i_{vscb}(\mathrm{r}-1) - d_2 i_{vscb}(\mathrm{r}-2) \tag{20}$$

$$i_{vscc}(\mathrm{r}) = n_o v_{ec}(\mathrm{r}) + n_1 v_{ec}(\mathrm{r}-1) + n_2 v_{ec}(\mathrm{r}-2) - d_1 i_{vscc}(\mathrm{r}-1) - d_2 i_{vscc}(\mathrm{r}-2) \tag{21}$$

Where, n_0,n_1,n_2,d_1 and d_2 are given in [24].

$$\text{And } v_{ea}(r) = v_{sa}^*(\mathrm{r}) - v_{sa}(\mathrm{r}) \tag{22}$$

$$v_{eb}(r) = v_{sb}^*(\mathrm{r}) - v_{sb}(\mathrm{r}) \tag{23}$$

$$v_{ec}(r) = v_{sc}^*(\mathrm{r}) - v_{sc}(\mathrm{r}) \tag{24}$$

Where, v_{sa}^*, v_{sb}^* and v_{sc}^* are the reference phase voltages and v_{sa}, v_{sb} and v_{sc} are sensed CCP phase voltages. CCP phase voltages are estimated through line voltages, which are expressed as,

$$v_{sa} = \frac{1}{3}\left(2v_{sab}^+ + v_{sbc}^+\right), \quad v_{sb} = \frac{1}{3}\left(-v_{sab}^+ + v_{sbc}^+\right), \quad v_{sc} = \frac{1}{3}\left(-v_{sab}^+ - 2v_{sbc}^+\right) \tag{25}$$

Where, v_{sab}^+,v_{sbc}^+ and v_{sca}^+ are line voltages as shown in Figs. 3-Figs. 5.

In an islanded control algorithm of VSC, the PR controllers give reference converter currents (i_{vsca}, i_{vscb} and i_{vscc}). The hysteresis current controller is used to generate the VSC switching pulses.

C. Modified Second Order Sequence (MSOS)–FLL based Synchronization Control

As shown in Figs. 5, the islanded DGS is transferred to the grid-connected mode, if the grid availability is assured. The theory behind the grid synchronizer process, is the estimation of grid voltages phase angles and islanded CCP voltages phase angles. The synchronization unit of DGS, is used to synchronize the phase islanded DGS voltages and phase angles of the grid voltages. The grid and CCP voltages phase angles are estimated through MSOS-FLL. The phase estimator algorithm is fast and capable to estimate the phase angles under distorted grid voltages. After the estimation of phase angles, a PI (Proportional Integral) controller is used, for matching of grid voltages and CCP voltages phase angles.

$$\Delta\theta_d(r) = \Delta\theta_d(r-1) + k_{ps}\{\theta_e(r) - \theta_e(r-1)\} + k_{is}\{\theta_e(r)\} \tag{26}$$

Where $\Delta\theta_d$ is the PI controller output and θ_e is the error of grid and standalone phase angle and it is expressed as,

$$\theta_e(r) = \theta_g(r) - \theta_s(r) \tag{27}$$

Where θ_g is the grid voltage angle and θ_s is the standalone voltage angle. The updated phase angle (θ_n) is given to the

This article has been accepted for publication in a future issue of this journal, but has not been fully edited. Content may change prior to final publication. Citation information: DOI 10.1109/TIA.2020.3021060, IEEE Transactions on Industry Applications

standalone controller for generating the standalone voltage same as the grid voltage as shown in Fig. 5. Hence the new updated phase angle is as,

$$\theta_n(r) = \theta_s(r) + \Delta\theta_d(r) \quad (28)$$

Where θ_s is the islanded CCP voltages phase angle.

IV. Results And Discussion

To demonstrate the effectiveness and robustness of the presented control, a DGS is developed in the laboratory as well as simulated in MATLAB/Simulink.

A. Performance of Microgrid in Simulation Platform

The fast and accurate phase angle information is necessary for fast synchronization of the islanded microgrid to the grid. MSOS-FLL also improves the reference grid current estimation performance because the unit vector information is used in the reference grid current estimation and the MSOS-FLL algorithm obtains it by estimating the positive sequence voltages from the unbalanced and distorted voltages. Fig.7 and Fig. 8 show the comparison of phase angle estimation performance at variable frequency using SRF-PLL, SOS-PLL and the MSOS-FLL. It is observed that at constant frequency, the performance of SRF-PLL, SOS-PLL and MSOS-FLL are similar. However, during the change in the frequency, the performance of MSOS-FLL is superior, and it is giving accurate phase angle information. Fig. 9 shows a comparison of synchronization performance using SRF-PLL and MSOS-FLL. It is observed that a synchronization of an islanded microgrid to the grid using MSOS-FLL is faster. Fig. 10(a) shows the seamless grid connection from an islanded to the grid connected mode. Fig. 10(b) shows the performance of the grid connected system at unbalanced load. Fig. 10(b) shows the battery current (I_b), grid current (i_g), load current (i_L), PV current (I_{pv}) and wind current (I_w). At unbalanced load, the battery current (I_b) is free from the second harmonic. Fig. 10(c) shows the response of DGS at solar insolation change and wind speed variation.

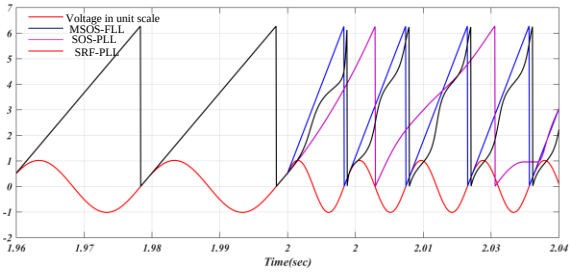

Fig. 7 Comparison of phase angle estimator of SRF-PLL, SOS-PLL and MSOS-FLL

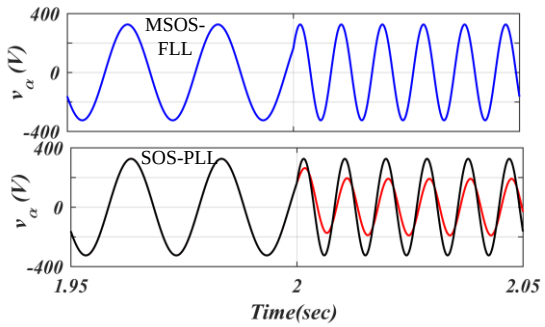

Fig. 8 Comparison of fundamental voltage estimation using MSOS-FLL and SOS-PLL during sudden frequency variation.

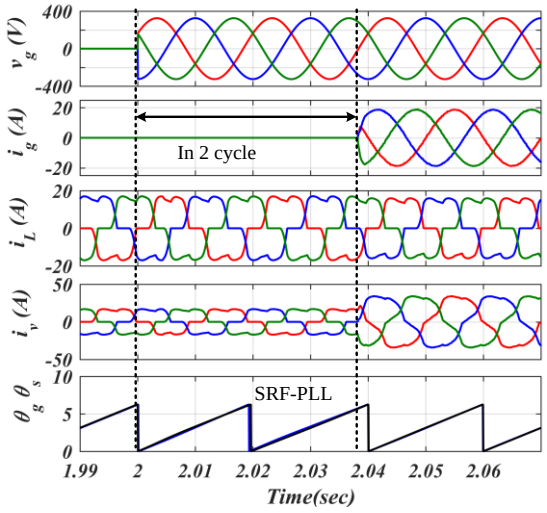

(a)

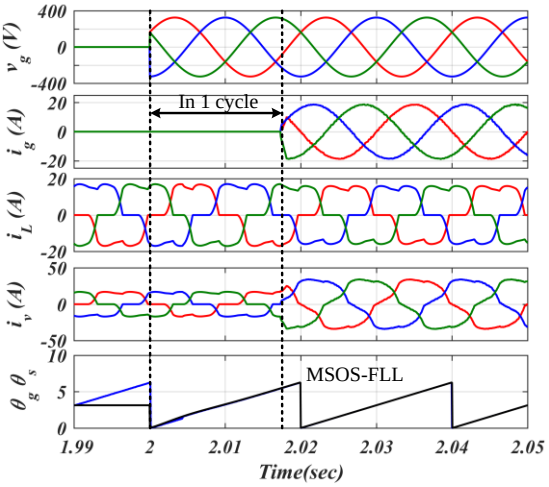

(b)

Fig.9 Performance of grid synchronization control (a) SRF-PLL based grid synchronization control (b) MSOS-FLL based grid synchronization control

B. Experimental Performance of DGS in Grid-Connected Mode

The rating of wind turbine driven generator is 230V, 50Hz, 1kW and the grid line voltage is 230V and 50Hz frequency. The solar PV rating is of 4.1kW with 400 V of an open circuit and 12 A of a short circuit current. The following subsections demonstrate test results at steady state and dynamics in the grid-connected mode, an islanded mode and during switching of modes. The performance of the DGS in steady state, is shown in Figs. 11-12. Here two RESs are used such as solar and wind-based energy. Therefore, the total generated power is 4.69kW (solar 4.2 kW and wind power is 0.59kW) as shown in Figs. 11-12. The load demand power is 2.00kW as shown in Fig. 12(c). The wind turbine driven SCIG current waveform shows the effectiveness of the machine converter, which is depicted in Fig. 12(a). In GC mode, the battery control comes into a constant current charging or discharging mode, which depends on the battery SOC (State of Charge). Here, the battery is only in constant current charging mode and its charging current is shown in Fig. 11(a). To balance the active power in DGS, the surplus power is injected into the grid at unity power factor. The injected grid current harmonics quality is 2.00%, which is under the IEEE-1547 and IEEE-519 standard. However, THD (Total Harmonic Distortion) of the load current is 23.00 % as shown in Figs. 12(g)-(i).

This article has been accepted for publication in a future issue of this journal, but has not been fully edited. Content may change prior to final publication. Citation information: DOI 10.1109/TIA.2020.3021060, IEEE Transactions on Industry Applications

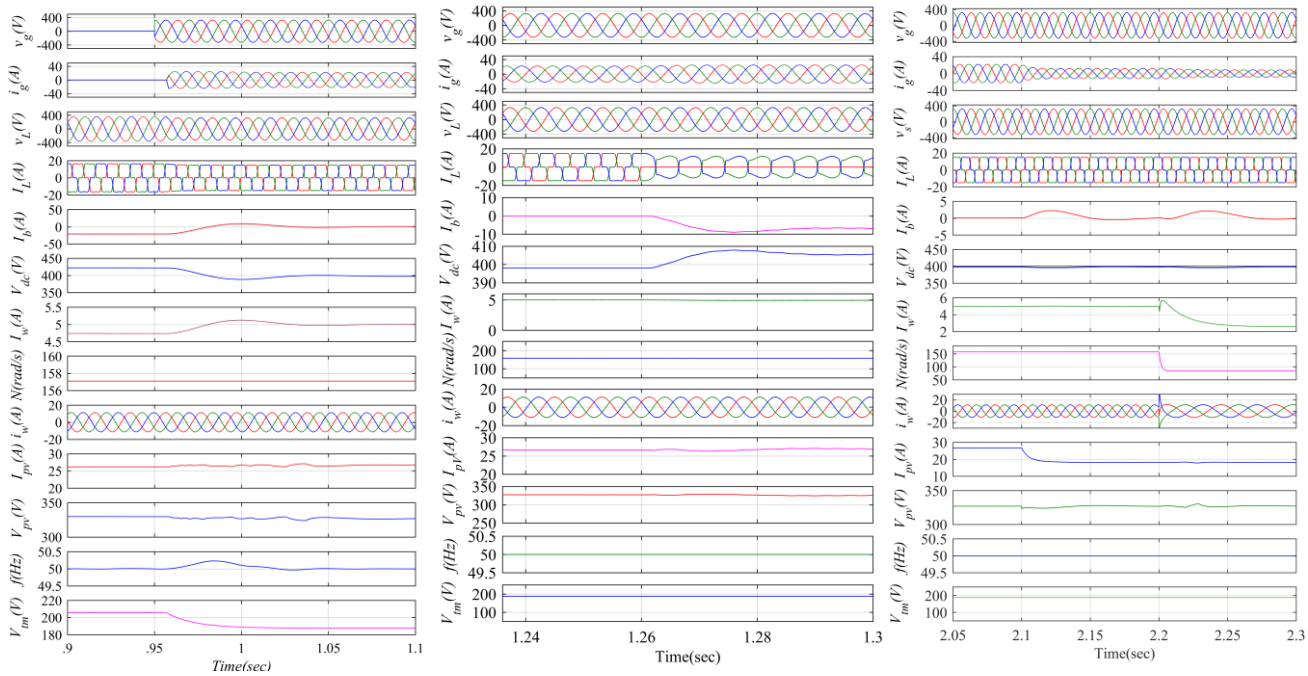

(a) (b) (c)

Fig. 10 Performance of DGS in simulation (a) grid synchronization (b) load unbalanced (c) solar insolation and wind speed variation

C. Dynamic Performance of DGS in Grid-Connected Mode

The improvement in dynamic performance of DGS, is depicted in Fig.13. The robustness of the grid connected control is presented at sudden solar power change in Fig. 13(a). Figs. 14(a)-(b) show the DC-link voltage and grid current transient with conventional feed-forward and with this feed- forward term. Here, it is observed that with this control, the DC-link voltage is maintained at similar value before and after the solar power transient. Similarly, the solar power irradiance changes from 1000W/m^2 to 500W/m^2 and vice versa is shown in Figs. 14(a)-(b) and at this condition, the grid current is smoothly changed, for balancing the active power in the DGS. Another dynamic condition is considered as, unbalanced load as shown in Figs.15 (a)-(b). The unbalanced load is realized at one phase load removal among the three phase load. At load unbalanced condition, the grid currents remain sinusoidal and balanced and it is accomplished through the LC control. As the one phase load is disconnected, the injected grid power is increased to balance the active power in the DGS. The load reactive power demand is also fulfilled by the VSC. Therefore, the grid current is always at unity power factor.

In grid-connected mode, the storage battery is controlled in constant current charging mode. If the battery is suddenly disconnected from the system as shown in Fig. 15 (c), the DGS operates in healthy condition. At the battery disconnection, the injected grid current is increased to balance the power and the grid current quality remains within the IEEE-1547 and IEEE-519 standards. Hence all dynamic conditions show the robustness and reliability of DGS in grid-connected mode.

D. Dynamic Performance of DGS in Islanded Mode

In an islanded mode of DGS, unbalanced load and solar irradiance dynamic conditions are observed in Figs.16 (a)-(c). Fig.16 (a) shows the one phase of load removal and at this load unbalanced condition, the CCP voltages remain sinusoidal. Subsequently, the power is balanced through the storage battery at load unbalanced condition as shown in Fig. 16(a). Therefore, the battery charging current is increased at one phase of load removal. Similarly, at load connection, the CCP voltage remains sinusoidal and the battery charging current is decreased.

The storage battery quickly responds as the solar irradiance is changed. The battery is used to maintain the active power balance in islanded DGS at solar irradiance change as shown in Figs. 16(b)-(c). The voltage and frequency are also regulated at varying solar irradiance, which is observed in Figs. 16 (b)-(c).

E. Performance of DGS in Mode of Switching

As the grid availability is assured by the synchronization unit, the DGS is reconnected to the grid as shown in Figs. 17(a)-(b). The robustness of the control strategy is observed from Fig.17 (a), which depicts the mode of switching from islanded to grid connected mode without any current and voltage transients. The load current is also not affected during mode of switching. As shown in Fig. 17(b), the STS signal is zero in an islanded mode and as the DGS comes into grid connected mode, the STS comes into one. During this mode of transition, the grid voltages and current are regulated with an improved quality. Moreover, Fig. 17 (a)-(b) show a comparison of MSOS-FLL and SOS-FLL based grid synchronization control. Performance of this MSOS-FLL is also shown in Fig. 17 (c) at distorted grid voltages.

F. Comparison of Grid Connected Control between Presented and Conventional Control Approaches

Fig. 18 shows the robustness of the grid connected control, which is based on IAPV, during the presence of DC-offset component in the load current.

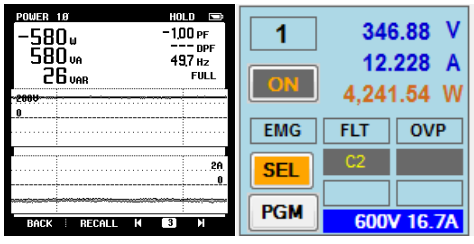

(a) (b)

Fig.11 Steady state performance of microgrid (a) battery power (b) solar power

This article has been accepted for publication in a future issue of this journal, but has not been fully edited. Content may change prior to final publication. Citation information: DOI 10.1109/TIA.2020.3021060, IEEE Transactions on Industry Applications

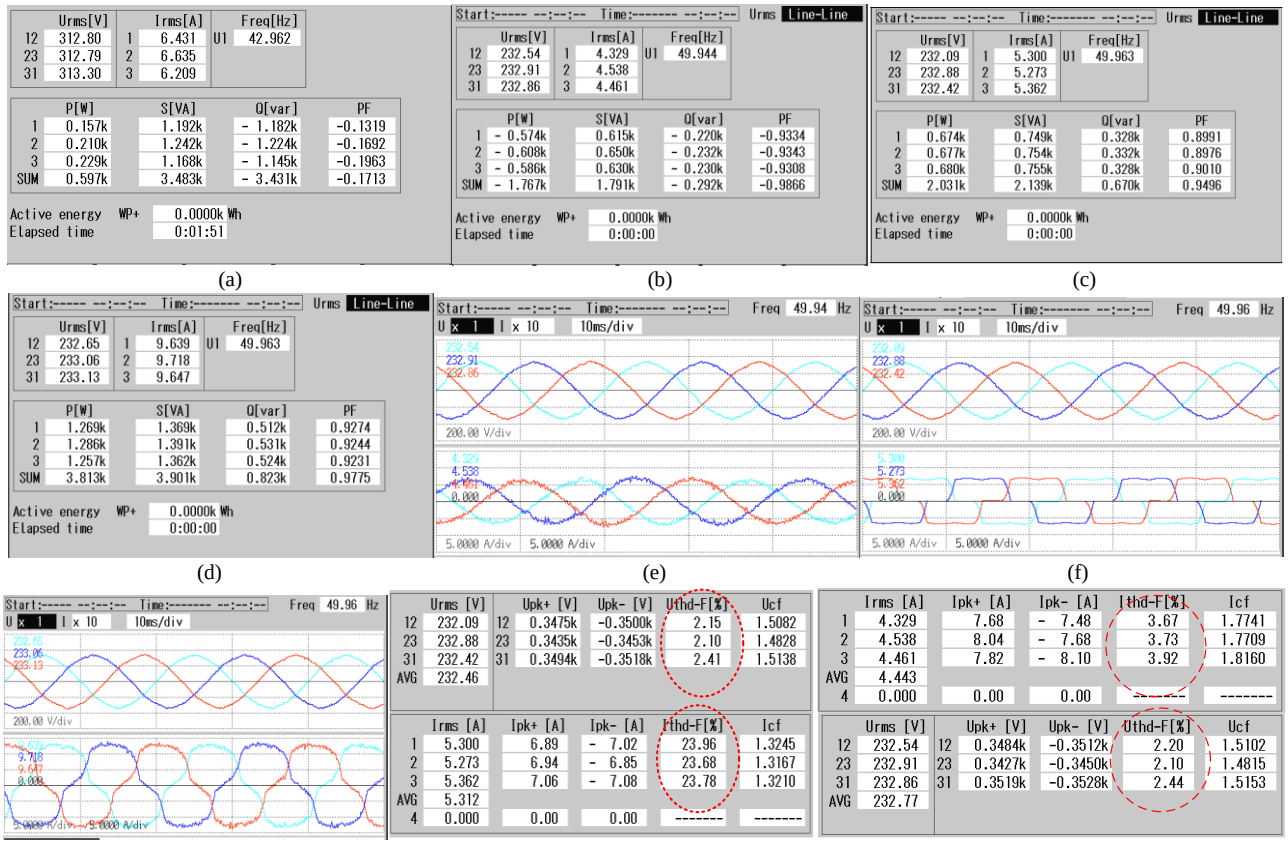

Fig. 12 Steady state performance of DGS in grid connected mode (a) P_w (b) P_g (c) P_L *(d)* P_{vsc} (e) *P_b (f) P_{pv} (g) v_{ccp}, i_g* (h) *v_{ccp}, i_L (i) v_{ccp}, i_{vsc} (j)* V_w and I_w (k) Harmonic spectrum of i_g and v_{ccp} (l) Harmonic spectrum of i_L and v_{ccp}

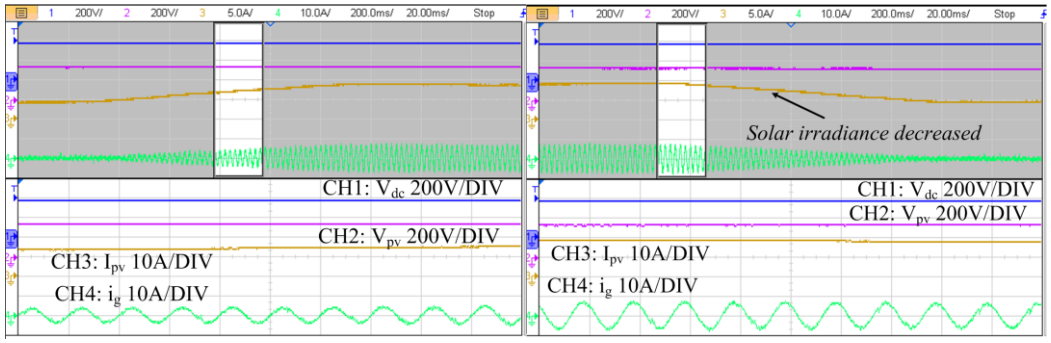

Fig.13 Dynamic performance of DGS in grid connected mode at solar irradiance change (a) V_{dc},V_{pv},I_{pv} and i_g (b) V_{dc},V_{pv},I_{pv} and i_g

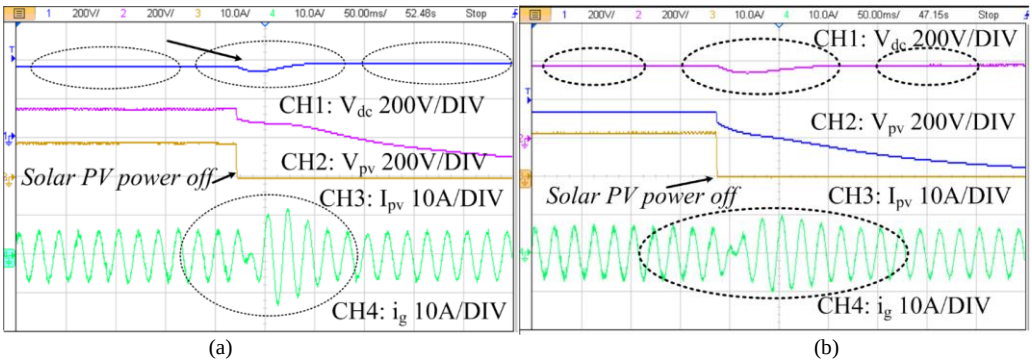

Fig. 14 Comparison of proposed control algorithm in grid connected mode with conventional (a) with feed-forward term (b) with presented feed-forward control.

This article has been accepted for publication in a future issue of this journal, but has not been fully edited. Content may change prior to final publication. Citation information: DOI 10.1109/TIA.2020.3021060, IEEE Transactions on Industry Applications

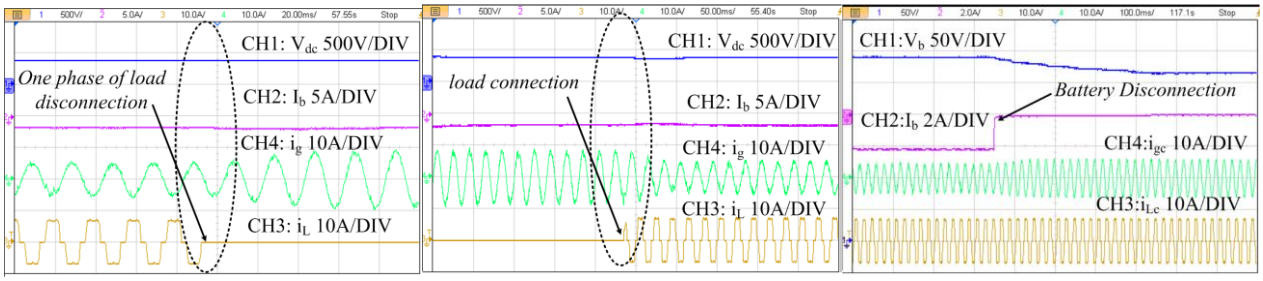

(a) (b) (c)

Fig. 15 Dynamic performance of DGS in grid connected mode at unbalanced load (a) v_{ccp} (c) P_g (d) v_{ccp}, i_L (e) Harmonic spectrum of i_L and v_{ccp} (f) P_L (g) P_{vsc} (h) v_{ccp}, i_{vsc} (i) V_w and I_w (j) P_w (k)V_b, I_b (j) P_b (m)MPPT at 1000W/m^2

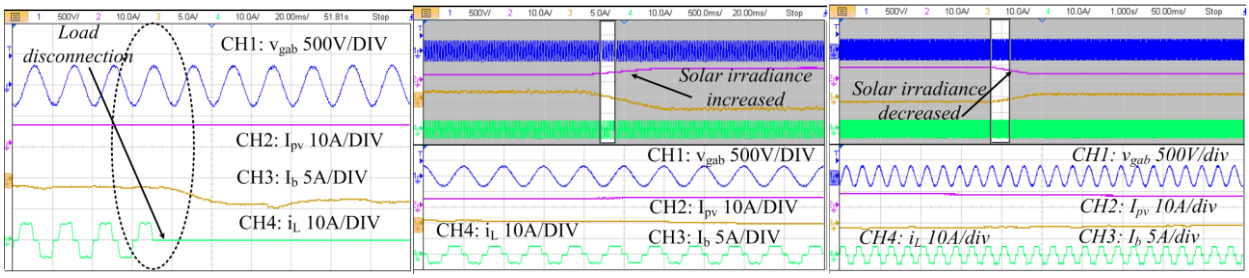

(a) (b) (c)

Fig. 16 Dynamic performance of DGS in islanded mode (a) *and* (b) *l*oad unbalanced (c) and (d) solar irradiance change.

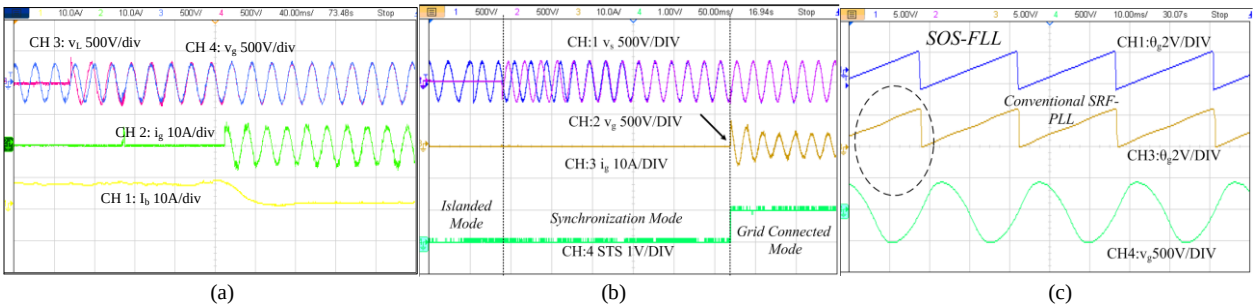

(a) (b) (c)

Fig. 17 Dynamic performance of DGS at mode of switching (a) v_s, v_g, i_g and i_L with proposed MSOS-FLL (b) v_s, v_g, i_g and STS with SOS-FLL and *(c)* v_g,θ_g (proposed SOS FLL) *and* θ_g (proposed conventional SRF-PLL)

As shown in Fig. 18 (a), the comparison of EPLL control with IAPV control for estimating fundamental load current. As depicted in Fig. 18 (a), fundamental load current estimation using IAPV control has good convergence and accurate rejection of DC-offset as compared to EPLL. Moreover, Fig. 18(b) shows a comparison of SOGI and other conventional LMS (Least Mean Square) control with presented IAPV control for fundamental load current estimation and Fig. 18(b) the superior and accurate, current estimation using IAPV as compared to other control algorithms

V. Conclusion

Performance of the DGS has been demonstrated for different modes of operation such as an islanded mode and the grid connected mode with the mode of switching. Test results show the robustness of control strategy, which is capable to operate in grid connected mode. Moreover, the transient free mode change is also presented through test results. The power quality of CCP voltages and currents, is also maintained within the IEEE-1547 standard, in the grid connected mode, an islanded mode and during the mode transitions. Test results have demonstrated the performance of DGS at different dynamic conditions and validated the robustness and effectiveness of control. Test results have also shown the effectiveness of feed-forward term in the grid connected mode and the smooth operation of the grid connected mode at a battery disconnection.

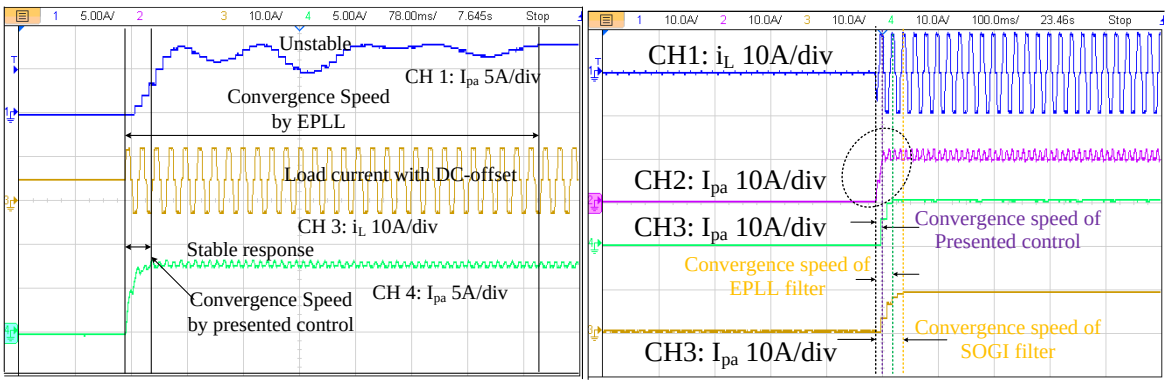

(a) (b)

Fig. 18 Comparison of grid connected control between presented and conventional control approaches with and without DC-offset condition.

ACKNOWLEDGEMENT

This work is supported by Indo-UK (RP03357); UKCERI-I (RP03391), FIST Project (RP03195) and JC Bose Fellowship.

REFERENCES

[1] Nikoobakht, J. Aghaei, M. Shafie-khah and J. P. S. Catalão, "Assessing Increased Flexibility of Energy Storage and Demand Response to Accommodate a High Penetration of Renewable Energy Sources," *IEEE Trans. on Sus. Energy*, Early Access, 2018.

[2] B. Celik, S. Suryanarayanan, R. Roche and T. M. Hansen, "Quantifying the Impact of Solar Photovoltaic and Energy Storage Assets on the Performance of a Residential Energy Aggregator," *IEEE Trans. Sus. Energy*, Early Access, 2018.

[3] G. Delille, B. Francois and G. Malarange, "Dynamic Frequency Control Support by Energy Storage to Reduce the Impact of Wind and Solar Generation on Isolated Power System's Inertia," *IEEE Trans. on Sust. Energy*, vol. 3, no. 4, pp. 931-939, 2012.

[4] I. Alsaidan, A. Khodaei and W. Gao, "Determination of battery energy storage technology and size for standalone microgrids," in *Proc. of IEEE, PESGM*, 2016, pp. 1-5.

[5] U. Datta, A. Kalam and J. Shi, "Battery Energy Storage System Control for Mitigating PV Penetration Impact on Primary Frequency Control and State-of-Charge Recovery," *IEEE Trans. Sus. Energy*, Early Access, 2018.

[6] Z. Yi, W. Dong and A. H. Etemadi, "A Unified Control and Power Management Scheme for PV-Battery-Based Hybrid Microgrids for Both Grid-Connected and Islanded Modes," *IEEE Trans. on Smart Grid*, vol. 9, no. 6, pp. 5975-5985, 2018.

[7] M. Jafari, Z. Malekjamshidi, J. Zhu and M. Khooban, "Novel Predictive Fuzzy Logic-Based Energy Management System for Grid-connected and Off-grid Operation of Residential Smart Micro-grids," *IEEE Jou. of Emer. and Sele. Top. in Power Elect.* Early Access, 2018.

[8] G. G. Talapur, H. M. Suryawanshi, L. Xu and A. B. Shitole, "A Reliable Microgrid with Seamless Transition Between Grid Connected and Islanded Mode for Residential Community With Enhanced Power Quality," *IEEE Trans. on Indu. Appl.*, vol. 54, no. 5, pp. 5246-5255, 2018.

[9] S. Adhikari and F. Li, "Coordinated V-f and P-Q Control of Solar Photovoltaic Generators with MPPT and Battery Storage in Microgrids," *IEEE Trans. on Sm. Grid*, vol. 5, no. 3, 2014.

[10] Q. Wu, E. Larsen, K. Heussen, H. Binder and P. Douglass, "Remote Off-Grid Solutions for Greenland and Denmark: Using smart-grid technologies to ensure secure, reliable energy for island power systems," *IEEE Electri. Magazine*, vol. 5, no. 2, pp. 64-73, 2017.

[11] S. S. Thale and V. Agarwal, "Controller Area Network Assisted Grid Synchronization of a Microgrid With Renewable Energy Sources and Storage," *IEEE Trans. on Sm. Grid*, vol. 7, no. 3, pp. 1442-1452, 2016.

[12] A. B. Shitole, Girish G. Talapur , Shelas Sathyan, Makarand S. Ballal, Vijay B. Borghate, Manoj R. Ramteke, Madhuri A. Chaudhari, "Grid Interfaced Distributed Generation System With Modified Current Control Loop Using Adaptive Synchronization Technique," *IEEE Trans. Ind. Infor.*, vol. 13, no. 5, pp. 2634-2644, 2017.

[13] D. Yazdani, A. Bakhshai, G. Joos and M. Mojiri, "A Nonlinear Adaptive Synchronization Technique for Grid-Connected Distributed Energy Sources," *IEEE Trans. Power Elect.*, vol. 23, no. 4, pp. 2181-2186, 2008.

[14] H. A. Hamed, A. F. Abdou, E. E. El-Kholy and E. H. E. Bayoumi, "Adaptive cascaded delayed signal cancelation PLL based fuzzy controller under grid disturbances," in *Proc. of IEEE MWSCAS*, 2016.

[15] A. Bouhouta, S. Moulahoum, N. Kabache and I. Colak, "Experimental Investigation of Fuzzy Logic Controller Based Indirect Current Control Algorithm for Shunt Active Power Filter," in *Proc. of IEEE International Conference on Renewable Energy Research and Applications (ICRERA)*, Brasov, Romania, 2019, pp. 309-314.

[16] W. Libo, Z. Zhengming and L. Jianzheng, "A Single-Stage Three-Phase Grid-Connected Photovoltaic System With Modified MPPT Method and Reactive Power Compensation," *IEEE Trans. Energy Conversion*, vol. 22, no. 4, pp. 881-886, Dec. 2007.

[17] K. Vishal and V. R., "An Improved SRF-Theory Based Controller Applied to Three Phase Grid Interfaced PV-System for Power Quality Improvement and Islanding Detection," in *Proc. of IEEE Innovative Smart Grid Tech. - Asia (ISGT Asia)*, Singapore, 2018, pp. 740-745.

[18] P. Chittora, A. Singh and M. Singh, "Adaptive EPLL for improving power quality in three-phase three-wire grid-connected photovoltaic system," *IET Rene. Power Gene.*, vol. 13, no. 9, pp. 1595-1602, 8 7 2019.

[19] A. Bendib, A. Chouder, K. Kara, A. Kherbachi and S. Barkat, "SOGI-FLL Based Optimal Current Control Scheme for Single-Phase Grid-Connected Photovoltaic VSIs with LCL Filter," in *Proc. of IEEE International Conference on Electrical Sciences and Technologies in Maghreb (CISTEM)*, Algiers, 2018.

[20] F. Xiao, L. Dong, L. Li and X. Liao, "A Frequency-Fixed SOGI-Based PLL for Single-Phase Grid-Connected Converters," *IEEE Tran. on Power Electr.*, vol. 32, no. 3, pp. 1713-1719, March 2017.

[21] T. Ngo, Q. Nguyen and S. Santoso, "Improving performance of single-phase SOGI-FLL under DC-offset voltage condition," in *Proc. of IEEE IECON 2014* , Dallas, TX, 2014, pp. 1537-1541.

[22] F. Huang, J. Zhang and S. Zhang, "Affine Projection Versoria Algorithm for Robust Adaptive Echo Cancellation in Hands-Free Voice Communications," *IEEE Trans. on Veh. Tech.*, vol. 67, no. 12, pp. 11924-11935, 2018.

[23] S. Kewat and B. Singh, "Grid Synchronization of WEC-PV-BES Based Distributed Generation System using Robust Control Strategy," in *Proc. of IEEE Ind. Appl. So. An. Meet.*, Baltimore, MD, USA, 2019, pp. 1-8.

[24] S. Pradhan, B. Singh, B. K. Panigrahi and S. Murshid, "A Composite Sliding Mode Controller for Wind Power Extraction in Remotely Located Solar PV–Wind Hybrid System," *IEEE Trans. Ind. Elect.*, vol. 66, no. 7, pp. 5321-5331, July 2019.

[25] F. Chishti, S. Murshid and B. Singh, "Development of Wind and Solar Based AC Microgrid With Power Quality Improvement for Local Nonlinear Load Using MLMS," *IEEE Trans. Industry Applications*, vol. 55, no. 6, pp. 7134-7145, Nov.-Dec. 2019.

[26] B. Singh, F. Chishti and S. Murshid, "Disturbance Rejection Through Adaptive Frequency Estimation Observer for Wind-Solar Integrated AC Microgrid," *IEEE Trans. Ind. Inf*, vol.15, no.11, pp. 6035-6047, 2019.

[27] P. S. Kumar, R. P. S. Chandrasena, V. Ramu, G. N. Srinivas and K. V. S. M. Babu, "Energy Management System for Small Scale Hybrid Wind Solar Battery Based Microgrid," *IEEE Access*,vol.8, pp.8336-8345, 2020.

[28] K. Kumar, N. Ramesh Babu and K. R. Prabhu, "Design and Analysis of RBFN-Based Single MPPT Controller for Hybrid Solar and Wind Energy System," *IEEE Access*, vol. 5, pp. 15308-15317, 2017.

[29] F. Chishti, S. Murshid and B. Singh, "LMMN-Based Adaptive Control for Power Quality Improvement of Grid Intertie Wind–PV System," *IEEE Trans. Industrial Informatics*, vol. 15, no. 9, pp. 4900-4912, Sept. 2019.

[30] S. Pradhan, S. Murshid, B. Singh and B. K. Panigrahi, "Performance Investigation of Multifunctional On-Grid Hybrid Wind–PV System With OASC and MAF-Based Control," *IEEE Trans. Power Electronics*, vol. 34, no. 11, pp. 10808-10822, Nov. 2019.

[31] A. A. A. Radwan and Y. A. I. Mohamed, "Grid-Connected Wind-Solar Cogeneration Using Back-to-Back Voltage-Source Converters," *IEEE Trans. Sustainable Energy*, vol. 11, no. 1, pp. 315-325, Jan. 2020.

[32] Y. M. Atwa, E. F. El-Saadany, M. M. A. Salama, R. Seethapathy, M. Assam and S. Conti, "Adequacy Evaluation of Distribution System Including Wind/Solar DG During Different Modes of Operation," *IEEE Transactions on Power Systems*, vol. 26, no. 4, pp. 1945-1952, Nov. 2011.

[33] S. L. Prakash, M. Arutchelvi and A. S. Jesudaiyan, "Autonomous PV-Array Excited Wind-Driven Induction Generator for Off-Grid Application in India," *IEEE Journal of Emerging and Selected Topics in Power Electronics*, vol. 4, no. 4, pp. 1259-1269, Dec. 2016.

[34] A. Parida and D. Chatterjee, "Model-based loss minimisation scheme for wind solar hybrid generation system using doubly fed induction generator," *IET Elec. Pow. App.s*, vol. 10, no. 6, pp. 548-559, 7 2016.

[35] M. Manohar, E. Koley and S. Ghosh, "Stochastic Weather Modeling-Based Protection Scheme for Hybrid PV–Wind System With Immunity Against Solar Irradiance and Wind Speed," *IEEE Systems Journal*.

[36] F. Giraud and Z. M. Salameh, "Steady-state performance of a grid-connected rooftop hybrid wind-photovoltaic power system with battery storage," *IEEE Trans. Energy Con.*, vol. 16, no. 1, pp. 1-7, March 2001.

[37] S. Kumar Tiwari, B. Singh and P. K. Goel, "Design and Control of Microgrid Fed by Renewable Energy Generating Sources," *IEEE Trans. Industry Applications*, vol. 54, no. 3, pp. 2041-2050, May-June 2018.

[38] S. Teleke, M. E. Baran, S. Bhattacharya and A. Q. Huang, "Rule-Based Control of Battery Energy Storage for Dispatching Intermittent Renewable Sources," *IEEE Trans. Sust. Ene.*, vol. 1, no. 3, pp. 117-124, Oct. 2010.

[39] R. G. Wandhare and V. Agarwal, "Novel Integration of a PV-Wind Energy System with Enhanced Efficiency," *IEEE Trans. Power Electronics*, vol. 30, no. 7, pp. 3638-3649, July 2015.

[40] B. Mangu, S. Akshatha, D. Suryanarayana and B. G. Fernandes, "Grid-Connected PV-Wind-Battery-Based Multi-Input Transformer-Coupled Bidirectional DC-DC Converter for Household Applications," *IEEE Journal of Emerging and Selected Topics in Power Electronics*, vol. 4, no. 3, pp. 1086-1095, Sept. 2016.

[41] A. Chatterjee and D. Chatterjee, "An Improved Current Balancing Technique of Two-Winding IG Suitable for Wind-PV-Based Grid-Isolated Hybrid Generation System," *IEEE Systems Journal*.

[42] C. Bhattacharjee and B. K. Roy, "Advanced fuzzy power extraction control of wind energy conversion system for power quality improvement in a grid tied hybrid generation system," *IET Generation, Transmission & Distribution*, vol. 10, no. 5, pp. 1179-1189, 7 4 2016.

[43] G. Ma, G. Xu, Y. Chen and R. Ju, "Multi-objective optimal configuration method for a standalone wind–solar–battery hybrid power system," *IET Renewable Power Generation*, vol. 11, no. 1, pp. 194-202, 11 1 2017.
[44] D. Lamsal, V. Sreeram, Y. Mishra and D. Kumar, "Kalman filter approach for dispatching and attenuating the power fluctuation of wind and photovoltaic power generating systems," *IET Generation, Transmission & Distribution*, vol. 12, no. 7, pp. 1501-1508, 10 4 2018.
[45] S. Singh, S. Kewat, B. Singh, B. K. Panigrahi and M. K. Kushwaha, "Seamless Control of Solar PV Grid Interfaced System With Islanding Operation," *IEEE Power and Energy Technology Systems Journal*, vol. 6, no. 3, pp. 162-171, Sept. 2019.
[46] H. Cha, T. Vu and J. Kim, "Design and control of Proportional-Resonant controller based Photovoltaic power conditioning system," in *Proc. of IEEE Energy Conversion Congress and Exposition*, 2009, pp. 2198-22

Seema (M'15) was born in Rampur, India, in 1989. She received B. Tech. degree in electrical engineering from Vivekanand Institute of Technology & Science, Ghaziabad, India, in 2010 and the M. Tech. degree in Electrical power management system from Jamia Millia Islamia, Delhi, India, in 2015. She is currently working toward the Ph.D. degree in Department of Electrical Engineering from Indian Institute of Technology, Delhi. Her areas of research interests include power electronics, renewable energy, micro-grid, power quality, and application of adaptive and robust control techniques in microgrid.

Bhim Singh (SM'99, F'10) was born in Rahamapur, Bijnor (UP), India, 1956. He received his B.E. (Electrical) from University of Roorkee, India, in 1977 and his M.Tech. (Power Apparatus & Systems) and Ph.D. from Indian Institute of Technology Delhi, India, in 1979 and 1983, respectively. In 1983, he joined Department of Electrical Engineering, University of Roorkee (Now IIT Roorkee), as a Lecturer. In December 1990, he joined Department of Electrical Engineering, IIT Delhi, as an Assistant Professor, where he has become an Associate Professor in 1994 and a Professor in 1997. He has been ABB Chair Professor from September 2007 to September 2012. He has also been CEA Chair Professor from October 2012 to September 2017. He has been Head of the Department of Electrical Engineering at IIT Delhi from July 2014 to August 2016. He has been the Dean, Academics at IIT Delhi from august 2016 to August 2019. He is JC Bose Fellow of DST, Government of India since December 2015. He is the Chairman of BOG of Maulana Azad National Institute of Technology, Bhopal, from 3rd July 2018. He is NonOfficial Independent Director, NTPC Limited, from 17th July 2018. He is also Governing Council Member of Central Power Research Institute, Banglore. He has guided 85 Ph.D. Dissertations and 168 M.E./M.Tech. /M.S.(R) thesis. He has filed 59 patents. He has executed more than eighty sponsored and consultancy projects. He has co-authored a text book on power quality: Power Quality Problems and Mitigation Techniques published by John Wiley & Sons Ltd. 2015. His areas of interest include solar PV grid systems, microgrids, power quality mitigation, PV water pumping systems, improved power quality AC-DC converters. He is a Fellow of Institute of Engineering and Technology (FIET), Institution of Engineers (India) (FIE), and Institution of Electronics and Telecommunication Engineers (FIETE). He is recipient of JC Bose and Bimal K Bose awards of The Institution of Electronics and Telecommunication Engineers (IETE) for his contribution in the field of Power Electronics. He has received 2017 IEEE PES Nari Hingorani Custom Power Award. He is also a recipient of "Faculty Research Award as a Most Outstanding Researcher" in the field of Engineering-2018 of Careers-360, India. He has received Academic Excellence Award-NPSC-2018. He has also received a Faculty Lifetime Research Award-2018 for overall research contribution at IIT Delhi.